

AD-752 465

MOLECULAR METAL LASER

Donald C. Lorents, et al

Stanford Research Institute

Prepared for:

Office of Naval Research
Advanced Research Projects Agency

27 November 1972

DISTRIBUTED BY:

NTIS

National Technical Information Service
U. S. DEPARTMENT OF COMMERCE
5285 Port Royal Road, Springfield Va. 22151

AD 752465

Semiannual Technical Report No. 1

November 27, 1972

Covering the Period April 15 to October 31, 1972

MOLECULAR METAL LASER

By: D. C. LORENTS, R. M. HILL, and D. J. ECKSTROM

Prepared for:

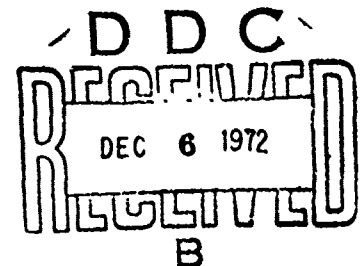
ADVANCED RESEARCH PROJECTS AGENCY
WASHINGTON, D.C. 20301

DIRECTOR, PHYSICS PROGRAMS, PHYSICAL SCIENCES DIVISION
OFFICE OF NAVAL RESEARCH
DEPARTMENT OF THE NAVY
800 NORTH QUINCY STREET
ARLINGTON, VIRGINIA 22217

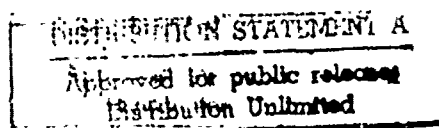
Sponsored by:

ADVANCED RESEARCH PROJECTS AGENCY
ARPA Order No. 1807, Program Code No. 2E90
CONTRACT N00014-72-C-0478 (15 April 1972-31 December 1972)
Contract Amount \$79,332 SRI Project PYU-1925

Reproduced by
NATIONAL TECHNICAL
INFORMATION SERVICE
U.S. Department of Commerce
Springfield VA 22151



STANFORD RESEARCH INSTITUTE
Menlo Park, California 94025 • U.S.A.



60

UNCLASSIFIED

Security Classification

DOCUMENT CONTROL DATA - R & D

Security classification of title, body of abstract and indexing annotation must be entered when the overall report is classified.

1. ORIGINATING ACTIVITY (Corporate author) Stanford Research Institute 333 Ravenswood Avenue Menlo Park, California 94025		2a. REPORT SECURITY CLASSIFICATION Unclassified	
		2b. GROUP	
3. REPORT TITLE Molecular Metal Laser			
4. DESCRIPTIVE NOTES (Type of report and inclusive dates) Semiannual Technical Report No. 1			
5. AUTHOR(S) (First name, middle initial, last name) Donald C. Lorents, Robert M. Hill, Donald J. Eckstrom			
6. REPORT DATE November 27, 1972		7a. TOTAL NO. OF PAGES 57	7b. NO. OF REFS 43
8a. CONTRACT OR GRANT NO. N00014-72-C-0478		9a. ORIGINATOR'S REPORT NUMBER(S)	
b. PROJECT NO. PYU 1925			
c.		9b. OTHER REPORT NO(S) (Any other numbers that may be associated with this report)	
d.			
10. DISTRIBUTION STATEMENT Distribution of this document is unlimited.			
11. SUPPLEMENTARY NOTES		12. SPONSORING/MONITORING AGENCY Advanced Research Projects Agency Order No. 1807, Program Code No. 2E90	
13. ABSTRACT This report describes theoretical and experimental research to determine the feasibility of an electron beam excited high-pressure Hg dissociation laser operating on the excimer continuum band. A model of the excitation, recombination, and molecular formation processes is presented. Experimental observations of the spectra in the 1-10 atm pressure range are presented, together with time decay studies of the continuum band. Details of illustrations in this document may be better studied on microfiche Ia			

DD FORM 1473

(PAGE 1)

PLATE NO. 21856

UNCLASSIFIED

Security Classification

S/N 0102-014-6600

Security Classification

KEY WORDS

LINK A

LINK 9

LINK C

ROLE

WT

[illegible]

WT

ROLE

WT

Ib



STANFORD RESEARCH INSTITUTE
Menlo Park, California 94025 · U.S.A.

Semiannual Technical Report No. 1

November 27, 1972

Covering the Period April 15 to October 31, 1972

MOLECULAR METAL LASER

By: D. C. LORENTS, R. M. HILL, and D. J. ECKSTROM

Prepared for:

ADVANCED RESEARCH PROJECTS AGENCY
WASHINGTON, D.C. 20301

DIRECTOR, PHYSICS PROGRAMS, PHYSICAL SCIENCES DIVISION
OFFICE OF NAVAL RESEARCH
DEPARTMENT OF THE NAVY
800 NORTH QUINCY STREET
ARLINGTON, VIRGINIA 22217

Sponsored by:

ADVANCED RESEARCH PROJECTS AGENCY
ARPA Order No. 1807, Program Code No. 2E90
CONTRACT N00014-72-C-0478 (15 April 1972-31 December 1972)
Contract Amount \$79,332 SRI Project PYU-1925

The views and conclusions contained in this document are those of the authors and should not be interpreted as necessarily representing the official policies, either expressed or implied, of the Advanced Research Projects Agency of the U.S. Government.

Approved by:

FELIX T. SMITH, *Manager*
Molecular Physics

CHARLES J. COOK, *Executive Director*
Physical Sciences Division

IC

CONTENTS

LIST OF ILLUSTRATIONS	iii
SUMMARY	1
I INTRODUCTION	4
II MODEL OF MOLECULAR FORMATION	6
III EXPERIMENTAL APPARATUS	11
IV EXPERIMENTAL OBSERVATIONS	18
Introduction	18
Atomic Spectra	19
Molecular Spectra	21
Analysis of Excimer Decay	24
V CONCLUSIONS	30
REFERENCES	31
APPENDICES	
A. MOLECULAR FORMATION IN ELECTRON-EXCITED HIGH PRESSURE RARE GASES	A-1
B. ELECTRON IMPACT CROSS SECTIONS FOR THE ELEMENT MERCURY	B-1

FIGURES

1	Molecular Energy Level Diagram for Hg_2 According to Finkelberg	9
2	Schematic of Hg Test Cell	12
3	Schematic of Test Setup	15
4	Overview of Test Setup	16
5	Time Histories of 4358 Å Radiation from Hg Following 3 nsec Excitation Pulse	20
6	Microdensitometer Traces of Hg_2 Molecular Continuum Spectra	23
7	Time History of Molecular Radiation at 4570 Å	25
8	Semilogarithmic Plot of Time History of Molecular Radiation at 4570 Å	26
9	Plot of Reciprocal of Intensity versus Time for Molecular Radiation at 4570 Å	28
A-1	Calculated Time Dependent Densities of Xe^+ , Xe_2^+ , Xe^0 and Xe_2	A- 8
B-1	Hg I Energy Levels from Tables of Moore	B- 3
B-2	Fits to Hg I Ionization Cross Section	B- 8
B-3	Total LCSS Function and eV/ion Pair for Mercury	B-11
B-4	Efficiencies for Deposition of Electron Energy into the 6^1P and 6^3P States of Mercury.....	B-12

SUMMARY

This report describes the status of a theoretical and experimental investigation aimed at development of a quantitative understanding of the mechanism of molecular radiation in high-pressure Hg and other diatomic metal systems to determine the feasibility of laser action in these systems. Mercury and other van der Waals molecules are promising candidates for laser action, because the molecular radiation is from a stable excited level to an unstable ground level that is always essentially unpopulated. Thus, a population inversion is readily achieved. Relatively high efficiencies of conversion of input energy to laser energy are also expected for van der Waals systems. On the other hand, since the molecular radiation is a continuum with a bandwidth on the order of hundreds of \AA , the optical gain is much smaller for a given population inversion than for comparable bound-bound transitions that have linewidths several orders of magnitude narrower.

We have directed our attention thus far to the study of Hg excited by a high-energy electron beam and in particular to its continuum radiation near 4800 \AA because of the potential applications of lasers at this wavelength. A theoretical model of the processes taking place in the gas, including the excitation, recombination, molecular formation, and relaxation processes, is presented in Section II. This model is based on information available from our past experience and from the literature and is similar to a kinetic model for the rare gases which is presented in Appendix A. Since little information is available on the rates of processes in Hg_2 , we are not yet able to make quantitative calculations using this model.

As one phase of our theoretical program, Professor A. E. S. Green at the University of Florida was subcontracted to calculate the

distribution of excitation energy in Hg. His preliminary report, presented in Appendix B, indicates that a majority of the energy is deposited in ions. The kinetic model describes the subsequent conversion of these ions to excited molecules.

The experimental program is described in Section III. Excitation of Hg vapor at pressures up to 10 atmospheres is provided by a 10-joule, 3 nsec pulse of 500 keV electrons from a Febetron 706. Experiments thus far include photographic and time-resolved emission spectroscopy of both atomic and molecular radiation. Results are described in Section IV. Most of the data have been obtained recently, and in many cases only qualitative observations are available. Some of these observations are:

- (1) For pressures above 1 atm, the atomic ions and highly excited atoms are channeled down to atomic levels with energies less than the molecular ionization level in times of a few nsec.
- (2) All excited atomic state populations disappear in times ranging from a few μsec at 1 atm to approximately 100 nsec at 10 atm.
- (3) The primary molecular continuum band extends from 3900 to 4900 \AA with the peak intensity near 4570 \AA . Secondary continua occur in the 5100-6000 and 3000-3600 \AA regions.
- (4) Molecular radiation at 4570 \AA persists for 10s of μsec and follows a nonexponential decay.

Analysis of the molecular radiation at 4570 \AA indicates that the transition has a radiative lifetime of approximately 20 μsec , and that the nonexponential behavior is due to deactivation during collisions of two excited molecules. The relatively long radiative lifetime and wide bandwidth of the Hg_2 continuum radiation lead to a very small optical

gain of 5×10^{-20} per cm per excited molecule/cm³, or 0.01/cm for 2×10^{17} molecules/cm³. Experiments and calculations are continuing to determine the feasibility of achieving excited molecule populations of this magnitude.

I INTRODUCTION

Developments in electron-beam and traveling wave discharge technology for excitation of high-pressure gases are having a major impact on the development of new lasers. The ability to inject energy rapidly into high-pressure gases, where collision processes are fast compared with radiative processes, opens up a new dimension for the development of lasers. It is possible under these circumstances to create inversions using new classes of reactions such as recombination, association, and energy transfer reactions. One class of molecules that has laser possibilities at high pressures is that known as van der Waals molecules. These molecules have basically repulsive ground states so that the unexcited gas consists of free atoms or loosely bound van der Waals molecules. In the excited gas, stable bound molecules (excimers) are formed from the association of an electronically excited atom and a ground state atom. At high pressures, these molecules rapidly relax to the bottom of their lowest bound excited electronic level and then radiate to the repulsive ground state which immediately dissociates. The repulsive ground state causes the emitted radiation to appear as a continuum band and allows the possibility of tuning over a portion of the band.

Although inversions are easily attained in these systems, the wide emission bandwidth means that large upper state populations are necessary to obtain a reasonable gain. Nevertheless, these media appear particularly promising for providing lasers of high efficiency, since every atom excited in the discharge forms an excited molecule that relaxes and then radiates. The efficiency, given by the ratio of the radiative transition energy to the mean excitation energy per atom, will generally be greater than 10%.

There are many possible candidates for such a laser medium, with transitions spanning the wavelength range from the vacuum uv to the infrared. These include the rare gases, Hg, Cd, Zn, and the alkaline earths. Carbone and Litvak¹ recognized the laser potential of the Hg₂ continuum band and attempted to obtain laser action on it using discharge excitation. Phelps² recently pointed out that various mixed gases such as rare gas-alkali combinations are also promising candidates.

In this report attention is focused on Hg. The interest in Hg stems from observations that the emission bands of this system are in the visible range. The so-called "4850 Å continuum" extends from 3800 to 6000 Å (the radiation in the 5500 Å region may be a separate continuum band), and a second continuum extends from 3000 to 3700 Å.³ We have devised a model of the excitation, recombination, association, and relaxation processes for Hg similar to that developed for Xe and Ar (see Appendix A). Unfortunately, the rate constants are not as well established in this case and the rate of formation of excited molecules cannot be reliably calculated. Therefore, most emphasis to date has been placed on the experimental measurements to obtain the molecular formation and decay rates. Our observations are preliminary and subject to confirmation by further measurements and data analysis. They do indicate that laser action in the "4850 continuum" may be possible but difficult to attain because of the long radiative lifetime and rapid collisional deactivation of the excimers.

II. MODEL OF MOLECULAR FORMATION

We present in this section a kinetic model for the excitation, ionic and molecular formation, and collisional and radiative relaxation of high-pressure Hg vapor excited by a pulsed electron beam. Since the reaction rates are not well known in Hg, we have patterned this model according to that of the rare gases given in Appendix A where the reaction rates are quite well known and the reaction chain is established. Although this model is quite general, the discussion refers to our experimental conditions, namely, to excitation by a 3 nsec pulse of 0.5 MeV electrons.

Because of the multiple scattering that occurs in the entrance window foil and in the high-density Hg vapor, the electron energy is deposited in a volume smaller than would be expected from the range of the electrons without scattering. Using multiple scattering theory, we have estimated the range of 0.5 MeV electrons in Hg at 10 atm to be about 1 cm. From the geometry of the incident beam, we estimate the excitation volume to be about 15 cm³, which together with the estimated energy delivered to the Hg (see Section III) gives an excitation energy of about 0.1 joule/cm³.

The energy deposition in Hg by the fast primary electrons is being considered by Bass, Berg and Green under a subcontract of this program, and their preliminary results are presented in Appendix B. The results show that, as in argon, the largest fraction of energy goes into ionization and that the 6¹P is the most strongly populated of the excited atomic states. Since the mean excitation energy per excited atom (excitation in this case includes ionization) calculated from the excitation efficiencies given in Appendix B is about 10 eV we obtain about 6×10^{17} excited atoms/cm³ produced by the electron pulse. An upper limit to the

radiative efficiency is obtained by assuming that every excited atom produces an excimer radiating at a mean energy of 2.7 eV. This efficiency limit is then 27%.

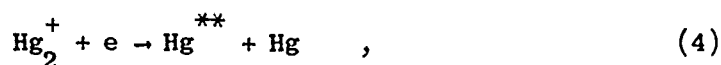
We now outline the mechanisms by which the energy of the electrons in the excitation pulse results in formation of the lowest lying excimers that are the upper level of the visible continuum radiation. In the initial process, the primary and secondary electrons produce excited atoms and ions by collision with ground state atomic Hg:



where Hg^{**} refers to excitation in any electronic level. As noted above, a majority of the excitation energy resides in the ions. These ions are converted to excited atoms in a two-step process. In the first step, the high atom density permits rapid formation of molecular ions through the three-body association reactions



In the second step, the molecular ions participate in fast dissociative recombination reactions with the electrons,



to produce an excited and a ground state atom.

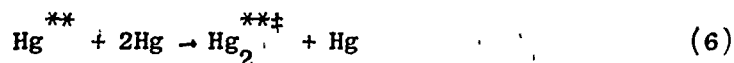
The excited atoms produced in reactions (1) and (4) that have energies greater than the energy of the molecular ion (8.6 eV according to Reference 4) can associatively ionize to Hg_2^+ by the process



All the atoms excited to levels lying above the 7^3P states are expected to participate in this associative ionization reaction and will cycle through Reactions (4) and (5) until they reside in a level below

that of the ion. Thus, by processes (3) through (5), all the ions and highly excited atoms created by the excitation pulse are converted to excited atoms in levels lying below the 6^3D state. These include the $6^1,^3P_{0,1,2}$, the $7^1,^3S$, and probably the $7^3P_{0,1}$ levels.

Formation of stable excited molecules from these excited atoms by the three-body associative reaction

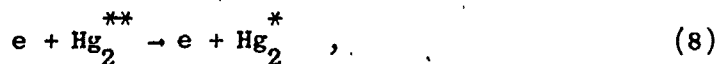


subsequently takes place, where the vibrationally-excited Hg_2^{***} may initially be in any of the molecular levels formed from the atomic states listed above. An energy level diagram for these levels as given by Finkelnberg⁵ is presented in Figure 1. Vibrational relaxation by the collisional process



will be rapid because of the possibility of atom exchange during the collision.

Electronic relaxation can occur via "curve crossings" or predissociation to lower atomic levels followed by reassociation into still lower molecular levels. This is believed to occur rapidly in Xe where the electronic levels are closely packed and many crossing interactions are possible; however in Hg, the levels are spaced more widely (see Figure 1) and the number of possibilities for curve crossing interactions is reduced so that relaxation by this process may be less effective. Relaxation can also occur by radiation and by collisions with electrons. The electrons cool rapidly by elastic and inelastic collisions to a temperature less than 1 eV. These electrons can absorb energy from the electronically excited molecules by the process

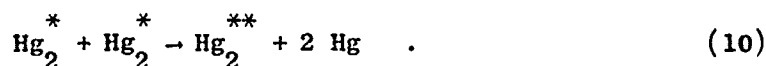


This process can be rapid enough to be of importance. In fact, at electron densities of 10^{16} and above, the electron collision processes almost certainly dominate the molecular relaxation. Rate constants for Reaction (8) estimated on the basis of similar processes in atoms range from 10^{-6} to 10^{-7} cm^3/sec , giving a decay time of 0.1 to 1 nsec at the above densities.

These electron-quenching and curve-crossing mechanisms funnel most of the molecules to the lowest stable excited $^3O_u^-$ level (see Figure 1), which is the upper level of the "4850 Å continuum." However, the electrons may also cause deactivation to the ground state by the process



thus reducing the efficiency of production of molecular radiators. At high molecular densities, another deactivation process may occur from the collision of two excited molecules, wherein one is deactivated to the ground state and the other absorbs the excess energy ("bi-excimer collisional deactivation"):



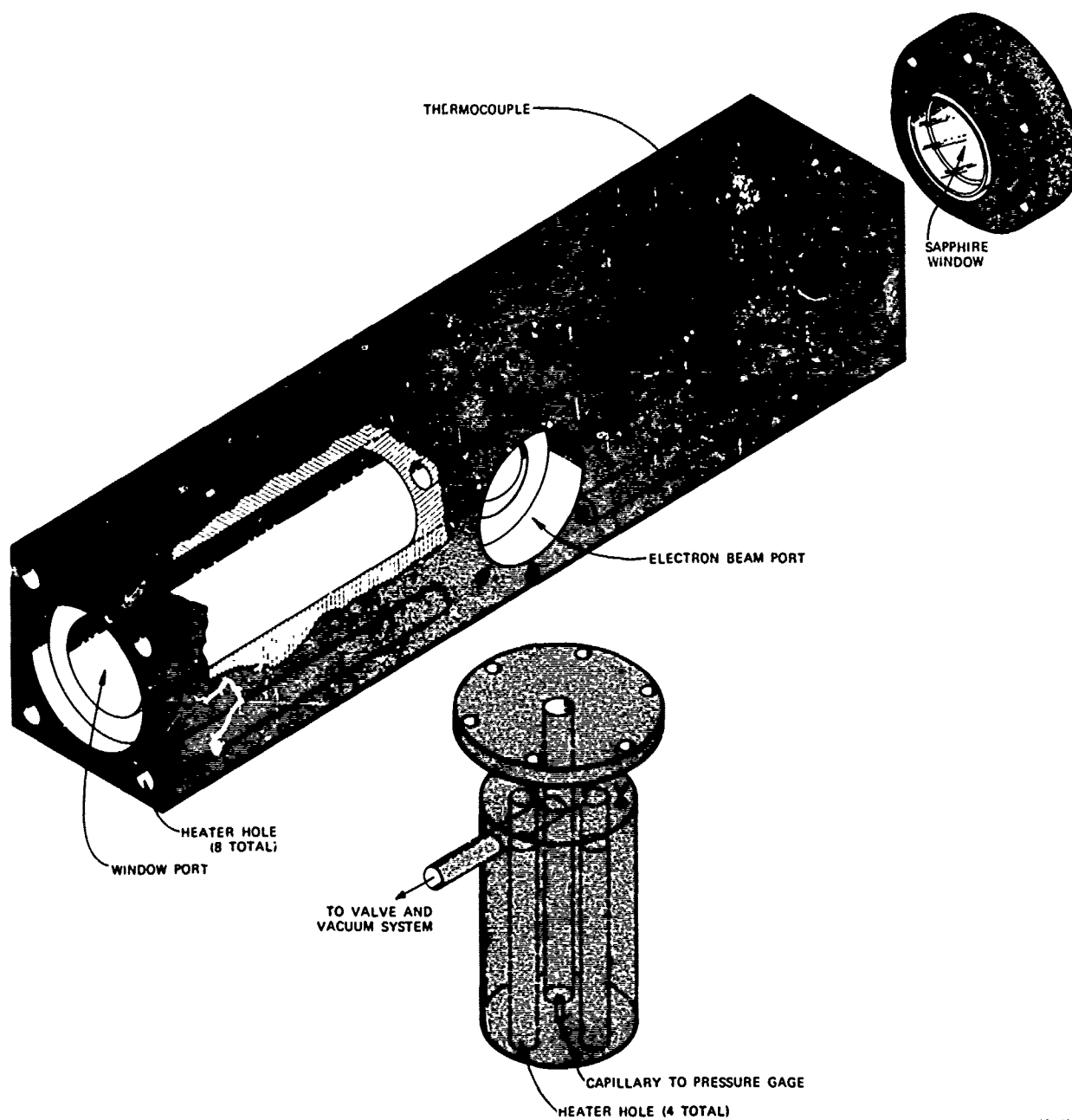
In a later section we present experimental evidence that indicates that Reaction (10) is indeed important as a deactivation process for Hg_2^* when the electron density is low.

III EXPERIMENTAL APPARATUS

The objective of the experimental program is to obtain information about the time histories of the populations of atomic and molecular states in high-pressure Hg vapor following an electron beam excitation pulse. From these time histories, we will determine rate constants and radiative transition probabilities that subsequently will be used in a kinetic model of the Hg_2 association laser. We are pursuing this objective by means of time-resolved emission and absorption spectroscopy of atomic and molecular transitions, as well as by time-integrated (photographic) spectroscopy. We are also preparing to measure the time history of ion concentration using a probe technique.

The high-pressure vapor is produced by heating a cell containing a reservoir of liquid Hg. The cell is fitted with optical windows for the spectroscopic measurements and with a foil window to admit the electron beam. The electron beam pulse is generated by a Febetron 706 (Field Emission Corporation, McMinnville, Oregon). According to the manufacturer's specifications, this machine produces a 2 cm^2 beam of 500 keV electrons at an average current of approximately 7000 amps. The total energy of the pulse is 10 joules and the pulse width is 3 nsec. We estimate that the electron beam diverges from 2 cm^2 to approximately 8 cm^2 over the distance from the Febetron face to the foil window and that about 50% of the energy is lost in the foil. Under these assumptions, approximately 1.5 joules of energy will be deposited in the gas. Taking the excited volume of gas as 15 cm^3 , this leads to the estimated excitation energy density of 0.1 joule/cm^3 given in the previous section.

The design of the test cell, shown schematically in Figure 2, for conducting spectroscopic studies on high-pressure Hg vapor excited by



SC-1925-7

FIGURE 2 SCHEMATIC OF Hg TEST CELL

an electron beam is a difficult problem for two reasons. First, the cell reaches temperatures up to 550°C , well above the temperature limit of elastomer and soft metal seals; and second, Hg vapor interacts with many metals in a deleterious manner. To overcome the reactivity problem, we have constructed most cell parts from low-nickel content Type 416 stainless steel. The optical windows at each end of the cell are 0.250 inches thick by 1 inch in diameter sapphire which are fused with a copper braze to stainless steel flanges. The electron beam window at the center of the cell is a disc of stainless steel of .004-inch thickness backed by a steel plate with 0.116-inch diameter holes (open area 55%). Beryllium was also tried for this window, but repeated flexing during alternate evacuation and pressurizing of the cell quickly produced cracks in this brittle material.

All joints are sealed by two concentric rings of wire. The inner ring is 0.005-inch diameter copper, while the outer ring is 0.008-inch diameter gold. The copper ring is less susceptible to interaction with the Hg, and the gold one, being larger and more ductile, forms a positive backup seal. Each wire is cut to length and laid in place with the ends overlapped, and the appropriate flange is then tightened in place. This system has been very satisfactory in preventing leaks, but the seals must be replaced occasionally because of amalgamation of the wires with the stainless steel cell at the highest temperatures of operation.

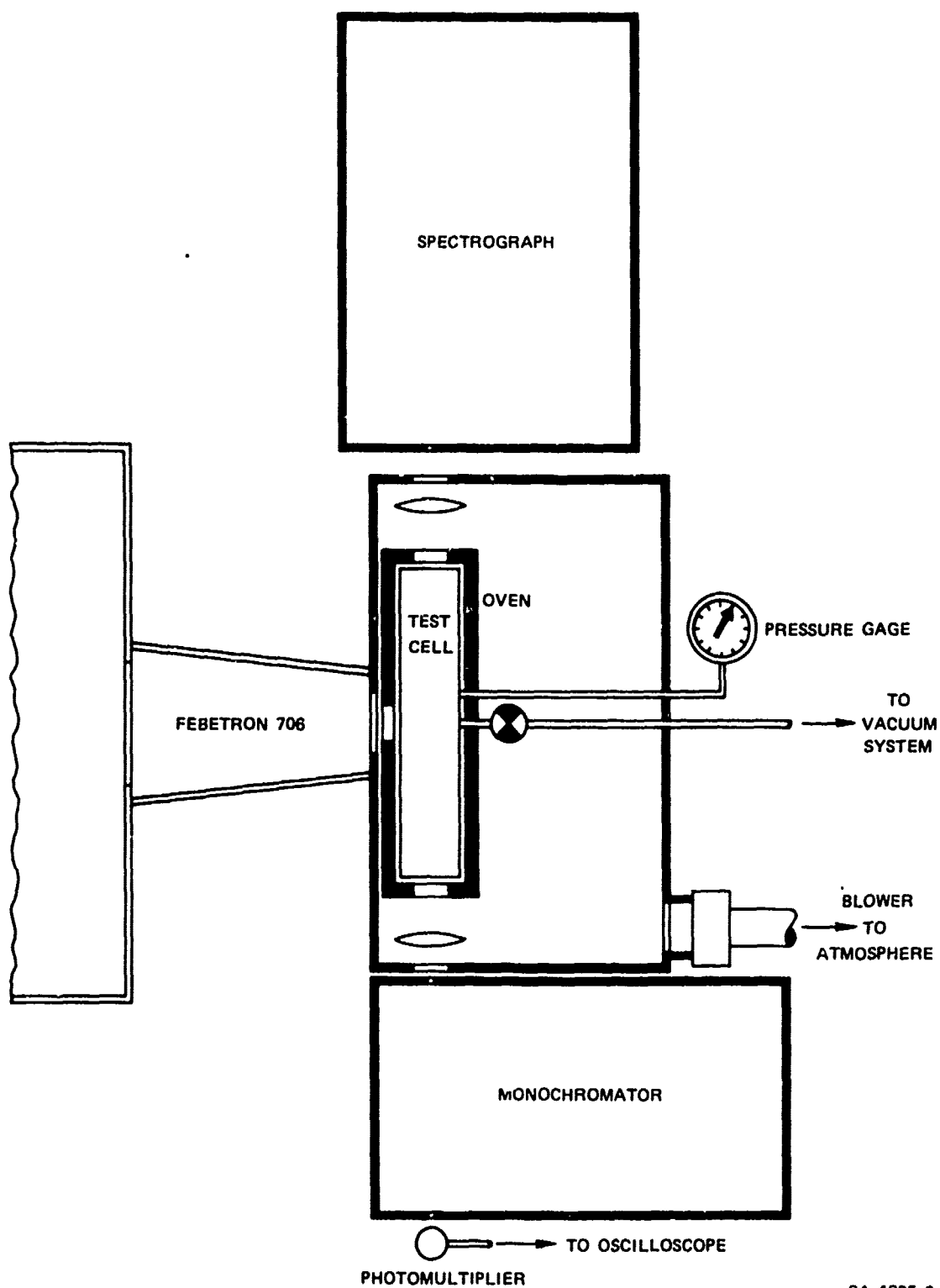
The cell, Hg reservoir, and valve are heated by a series of Hotwatt cartridge heaters. Eight heaters are placed in holes drilled in the cell, four more in holes drilled in the reservoir, and two in a copper block that surrounds the valve. The entire apparatus is enclosed in an insulating oven constructed from 1-inch maranite with appropriate openings for the optical and electron beams. Thermocouples monitor cell and reservoir temperatures. In operation the reservoir is maintained approximately 20°C cooler than the cell at all times to ensure that

condensation of the Hg occurs only in the reservoir. It was originally intended that the vapor pressure be deduced from the reservoir temperature, but uncertainties about condensation at unexpected cool points in the system led us to seek a direct pressure readout. This was accomplished by adding a small capillary tubing from the bottom of the reservoir leading to a Foxboro bourdon tube pressure gauge. The system was evacuated, and the entire gauge, capillary, and reservoir system was filled with Hg. Calibration of this system against a gas-filled gauge established its accuracy to $\pm 1\%$ over the range from 0 to 200 psia.

When conducting tests, the cell is evacuated to the vapor pressure of Hg, sealed off, and heated. Several square centimeters of titanium-zirconium alloy (Oregon Metallurgical Corp., Albany, Oregon) present in the cell at all times act as a getter for N_2 , O_2 , H_2O , and other impurities that may be present in the cell (no impurity spectra have been observed in our studies to date).

The cell system and oven are enclosed in a wooden box lined with 1/4-inch lead sheet for protection from X-rays produced by the electron beam pulse, as well as for confinement of possible Hg leaks. A blower draws air from this box and expels it outside the building to reduce the possibility of Hg vapor in the room air. Apertures in the box are provided for the optical and electron beams. The test layout is shown schematically in Figure 3 and photographically in Figure 4.

Spectroscopic measurements have been made using a Heath Model 700 grating monochromator, a Hilger 1/4-meter quartz prism spectrograph, and a McPherson Model 216.5 1/2-meter grating spectrograph. Time-resolved monochromatic measurements utilize an RCA 1P28 photomultiplier (PM) and either a Tektronix Model 551 or a Hewlett Packard Model 183A oscilloscope. We have experienced some difficulty with nonlinearity and saturation of the PM caused by large current pulses. It appears that this



SA-1925-6

FIGURE 3 SCHEMATIC OF TEST SETUP

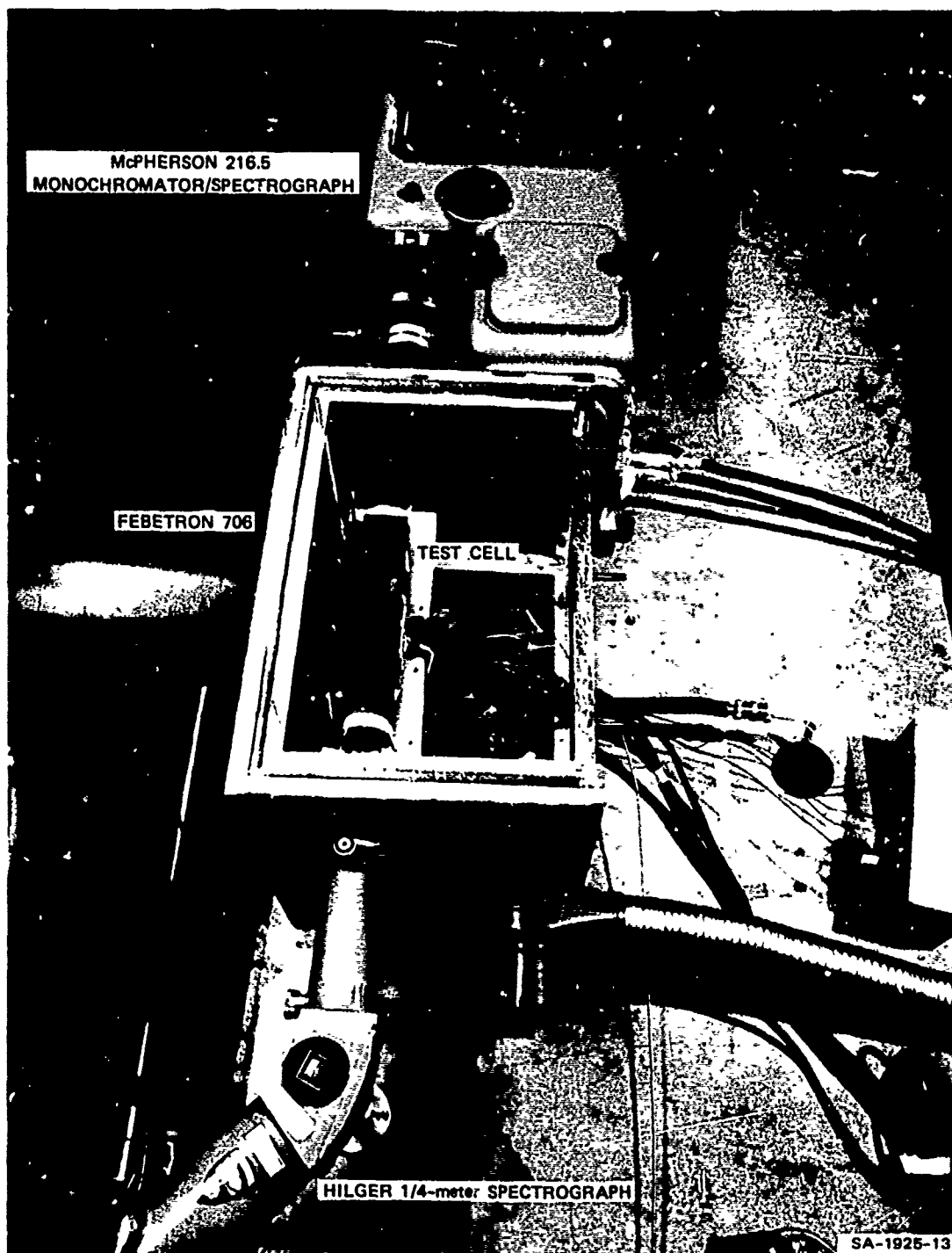


FIGURE 4 OVERVIEW OF TEST SETUP

problem is eliminated by reducing the light intensity so that the maximum current is kept below 2 mA. The noise signal produced by the 3-nsec electron beam pulse is reduced by shielding the cables and PM from rf and X-ray-induced signals and by operating the scopes in a shielded room. The noise signal is still visible on the highest sensitivity scales but is no longer than the beam pulse and has not become a problem.

Because of the large amount of data expected to be gathered in the form of oscilloscope records, we have automated the data reduction process insofar as possible. Polaroid photographs of the oscilloscope traces are read on a digitizing instrument that records x,y coordinates on either IBM cards or magnetic tape. These points for each case are then used to produce computer-generated plots of any form desired. The computer program is currently being upgraded to include least-squares curve-fit routines for the determination of various rates and time constants.

IV EXPERIMENTAL OBSERVATIONS

Introduction

The expected qualitative behavior of the Hg vapor was discussed in the earlier section on the kinetic model. Since all states with energies higher than that of the molecular ion, Hg_2^+ , are believed to be rapidly quenched, we expect at the higher pressures to see atomic radiation only from atomic levels that can be fed by Reaction (4), i.e., states that have energies of less than 8.6 eV. These include the 7S and 6P singlet and triplet states. We do in fact observe strong radiation from the 7^3S_1 level (4047, 4358, and 5461 Å) and relatively much weaker radiation from the 7^1S_0 level (4078 Å). Radiation from $6^3\text{D} - 6^3\text{P}$ at 3126 and 3650 Å is strong at pressures below a few hundred torr. At higher pressures, this radiation becomes much weaker, being several orders of magnitude below the radiations from 7^3S . Since the 6^3D level lies at 8.8 eV this confirms that associative ionization [Reaction (5)] is occurring rapidly and is consistent with a molecular ion level of 8.6 eV. Radiation from the 6P levels to the ground state is completely trapped and not observed.

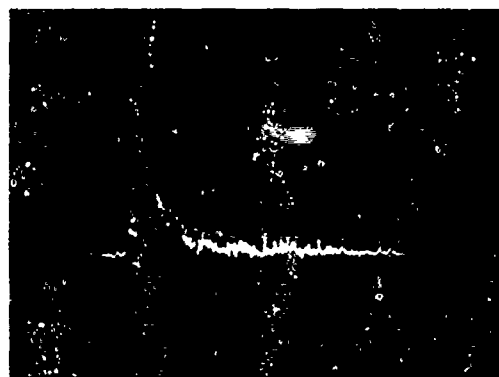
The molecular state structure for Hg_2 is not well established, and the identification of various bands with particular transitions is uncertain. We are most interested in the continuum band centered near 5000 Å, which presumably originates from the $^3\text{O}_u^-$ level formed by $6^1\text{S} + 6^3\text{P}_0$ atomic states. A second continuum band centered around 3300 Å and presumed to originate from the $^3\text{I}_u$ level ($6^1\text{S} + 6^3\text{P}_1$) is also well known. In addition, Takeyama (see Rosen³) has identified as many as 12 band systems that cover the 3000 to 5400 Å wavelength range, and it is not clear whether these systems are resolved parts of the two continua

or whether they originate from bound-bound transitions of upper molecular (or possibly ionic) levels.

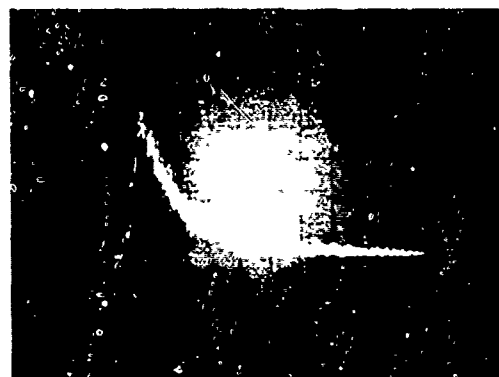
In our experiments to date we have measured as a function of Hg pressure the time-resolved emissions at 4358 Å as representative of the atomic $7s^3S_1$ level, and at 4570 and 3300 Å as representative of the two molecular continua. These experiments cover the pressure range from approximately 1 to 10 atm. We have also done a limited number of absorption experiments using the 4047 Å atomic Hg line in an attempt to deduce the 6^3P_0 population history. In addition, we have taken photographic spectra over the range from approximately 2500 to 6000 Å to determine the overall features of the radiation. The results of these experiments are discussed in the following paragraphs.

Atomic Spectra

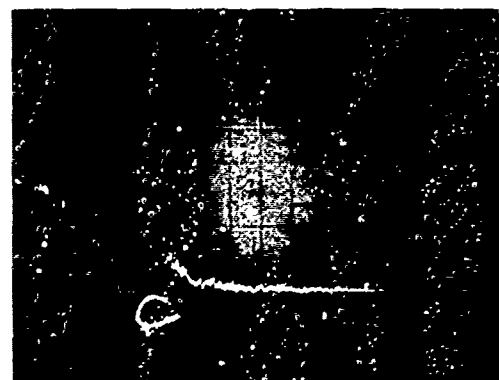
As noted above, at high pressures significant atomic spectra were observed only from the 7^3S_1 state, implying that atoms in higher states are quenched rapidly through Reactions (4) and (5). Characteristic time-resolved emission histories at 4358 Å for three different pressures are shown in Figure 5. At the lowest pressure of 1 torr where collision processes are slow (Figure 5a) the emission decays exponentially with the 30-40 nsec lifetime characteristic of the 7^3S_1 state. At an intermediate pressure of 250 torr (Figure 5b), the emission initially decays exponentially due to 7S states directly populated by the electron pulse, but then rises to a second maximum due to funneling of excitation energy into the 7S levels from ion recombination. For the highest pressure case of 7700 torr (Figure 5c), the production of 7S states by ion recombination is very fast and is not distinguishable from the direct excitation. The rate of decay of the 7^3S_1 level is now increased because the rate of molecular formation has become comparable with the radiative decay rate.



(a) 1 torr, 50 nsec/cm



(b) 250 torr, 200 nsec/cm



(c) 7700 torr, 50 nsec/cm

SA-1925-9

FIGURE 5 TIME HISTORIES OF 4358 Å
RADIATION FROM Hg
FOLLOWING 3 nsec
EXCITATION PULSE

The peak intensity of the 4358 Å radiation shown in Figure 5 increases with increasing pressure, but rapid depletion of the 7³S state causes the integrated atomic radiation intensity to decrease with increasing pressure above several atm. This is also shown in microdensitometer traces of photographic spectra which are presented below.

We tried to monitor the population of the 6³P levels by the absorption of line radiation from an external source of mercury light. Observation of the time dependence of these populations as a function of pressure could provide rate constants for Hg₂^{*} formation from these states. We used an intense, dc, mercury arc as the source of line radiation and the McPherson monochromator as a filter and detector. We observed no absorption at any pressure. The beam excited radiation from the 7³S states was initially much larger than the intensity of the dc arc, so that absorption could have been seen only at times later than the decay of the light produced by the beam pulse. The decay of this light was a function of pressure (Figure 5) so that the absorption observations were limited to times $t > 5 \mu\text{sec}$ at 1 atm decreasing to $t > 100 \text{ nsec}$ at 10 atm.

We estimate that a 6³P population of $10^{13}/\text{cm}^3$ would have been readily observable, so that a negative result places some definite limits on Hg₂^{*} formation. Either Hg₂^{*} is formed from states other than the 6³P atomic states and very little energy even reaches these levels, or the Hg₂^{*} formation rate from the 6³P states is at least as fast as the reaction depleting the 7³S level, which is also assumed to be molecular formation to Hg₂^{**}. Measurements of molecular state population will help to resolve this.

Molecular Spectra

In our molecular spectrum studies to date, we have concentrated on the continuum near 4800 Å as the region of greatest interest for Hg

laser studies. Microdensitometer traces of typical photographic spectra taken with the McPherson grating instrument at three different pressures are presented in Figure 6 (each spectrum was exposed for five Febetron pulses, and the vertical scale is shifted for each trace). These spectra cover the 4000 to 5000 Å range, with essentially linear dispersion. The major features to note are:

- (1) The band extends from 3900 to 4900 Å, with the peak intensity around 4570 Å.
- (2) The width and shape of the band are essentially independent of pressure, although there is some flattening of the peak at higher pressures.
- (3) There is evidence of structure on the continuum at the lower pressures which disappears at higher pressures.
- (4) The 7^3S atomic radiation at 4047 and 4358 Å decreases in absolute intensity and relative to the molecular radiation as the pressure increases above 1 atm.

Photographic spectra taken with the Hilger prism instrument, which cover the range from 2500 to 6000 Å, also show a continuum over the wavelength range from 5100 to 6000 Å with a peak in the vicinity of 5400 Å, which is continuous with, but much weaker than, the 4500 Å continuum. Although instrument and film responses have not been calibrated, the 3300 Å continuum is also observed to be very much weaker than either of the two visible bands. The relative weakness of 3300 Å radiation has been substantiated by photomultiplier measurements.

Prior observations of the Hg_2 continuum going back more than 80 years led us to expect two broad bands peaking near 3300 Å and 4850 Å, with radiation extending up to 6000 having a secondary peak near 5200 Å. Therefore, we were surprised to find the main peak in our

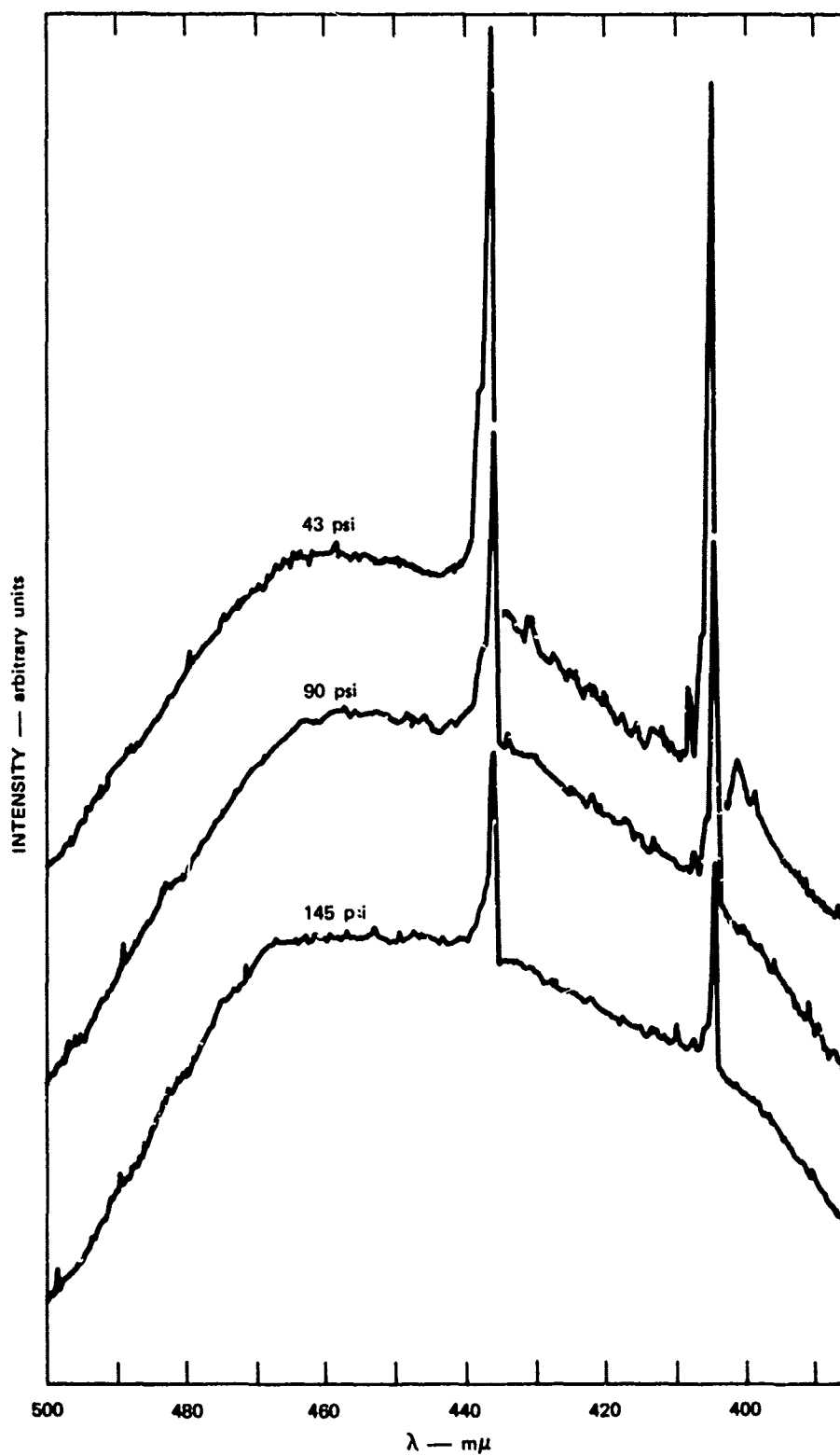


FIGURE 6 MICRODENSITOMETER TRACES OF H₂ MOLECULAR CONTINUUM SPECTRA.
Note shift of zero level for each curve.

experiments to occur near 4570 \AA . Rosen's tables³ revealed that Takeyama had observed a molecular band that peaked near 4550 \AA , which may be the same radiation that we observe. The band structure observed at lower pressure, Figure 6a, has peaks that agree well with some of those listed by Takeyama. These bands appear to quench or broaden as the pressure increases without shifting the basic form of the observed radiation. We can conclude only that electron beam excited Hg_2 spectra, ours and Takeyama's, are distinctly different from those of prior observations, mostly excited by 2537 \AA absorption. We are going to try to observe the Hg_2 states by absorption measurements, using short, intense white light sources and looking for absorption bands. Data of this type would be very helpful in unscrambling the present state of confusion about the Hg_2 molecular spectra.

We have taken a large number of time histories of emission at the peak of the molecular continuum at 4570 \AA . A typical oscilloscope trace is shown in Figure 7, and a semilog plot (of a different run) is shown in Figure 8. These figures are typical of data taken over the pressure range from 1 to 10 atm. Three points are noteworthy:

- (1) The rise time is very rapid, on the order of 10s of nanoseconds.
- (2) The duration of radiation is 10s of microseconds.
- (3) The decay is nonexponential over the range of times observed thus far.

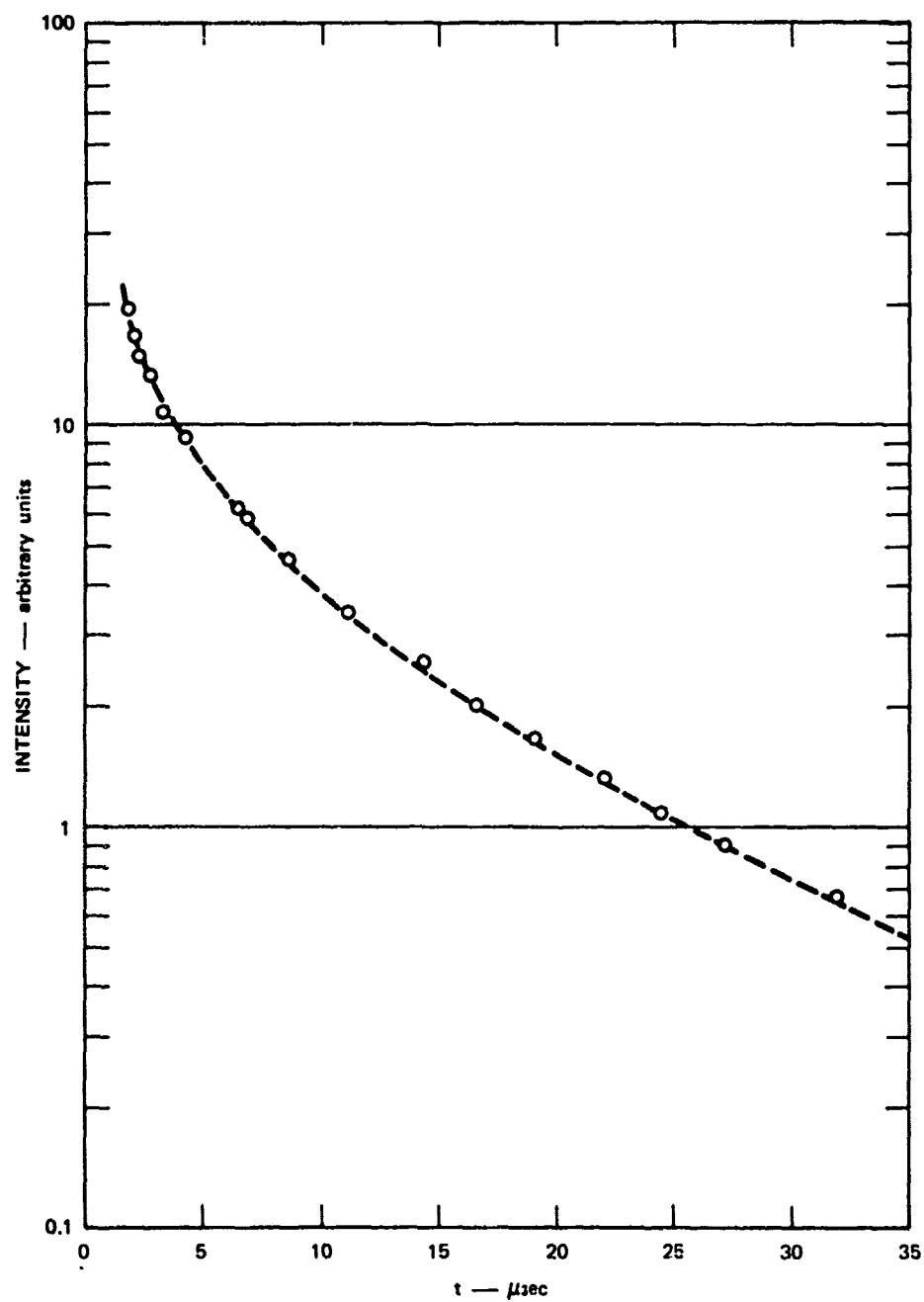
These observations indicate that the molecular formation is very rapid and that the radiative lifetime of the molecular level is relatively long.

Analysis of Excimer Decay

We suggest that the nonexponential decay of the 4570 \AA radiation is caused by bi-excimer collisional deactivation of the Hg_2^* level by



FIGURE 7 TIME HISTORY OF MOLECULAR RADIATION
AT 4570\AA (PRESSURE = 5400 torr, $1\text{ }\mu\text{sec/cm}$)



SA-1925-11

FIGURE 8 SEMILOGARITHMIC PLOT OF TIME HISTORY OF MOLECULAR RADIATION AT 4570Å (PRESSURE = 5270 torr)

Reaction (10). If this is the dominant reaction taking place, the rate equation is simply

$$\frac{dN^*}{dt} = -k(N^*)^2, \quad (11)$$

where N^* is the population of Hg_2^* , which has the solution

$$\frac{1}{N^*} = \frac{1}{N_0^*} + kt. \quad (12)$$

Since the intensity is directly proportional to N^* , a plot of $1/I$ versus t should produce a linear curve. Two such plots are presented in Figure 9 for two different pressures. The curves are linear for at least $10 \mu\text{sec}$, and both curves have the same slope representative of the rate constant k , strongly supporting the above hypothesis.

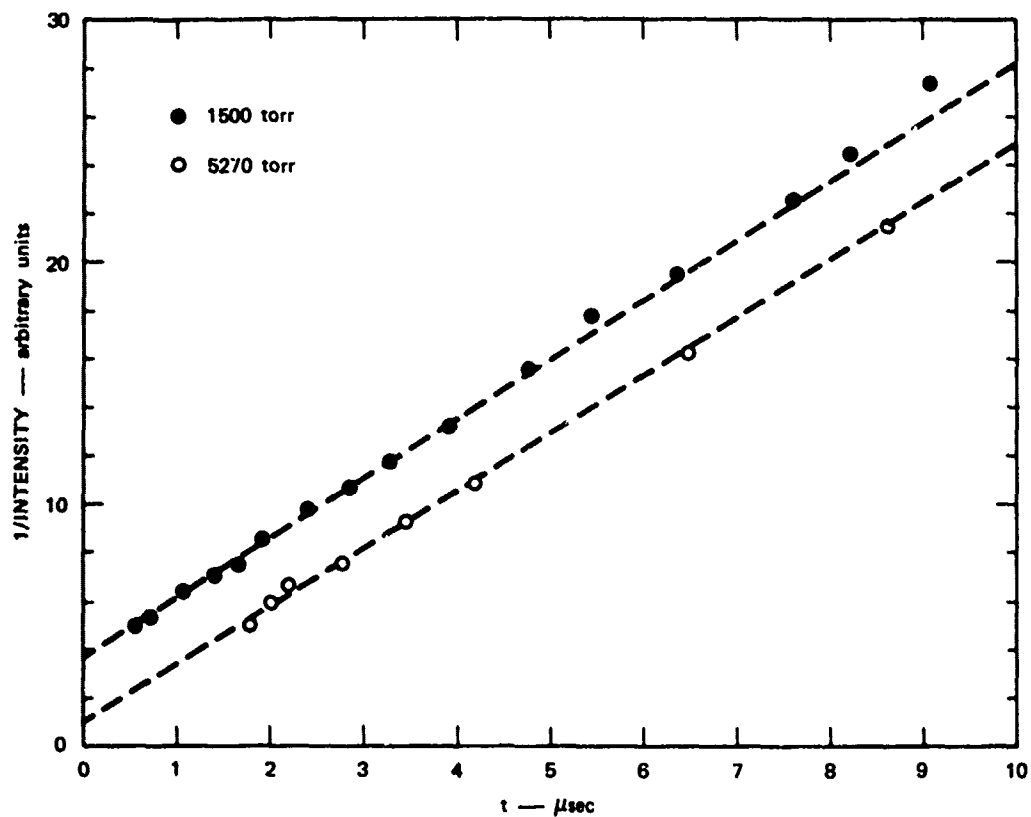
If we also include spontaneous emission in the rate equation, it becomes

$$\frac{dN^*}{dt} = -k(N^*)^2 - \lambda N^*, \quad (13)$$

where λ is the radiative transition probability. This has the solution

$$\frac{N_0^*}{N^*} = \left(\frac{kN_0^*}{\lambda} + 1 \right) e^{\lambda t} - \frac{kN_0^*}{\lambda}, \quad (14)$$

which describes the decay as it becomes dominated by the radiative term. In Figure 8, the data of Figure 9 at 5270 torr are shown, together with a curve representing Equation (14) with the parameters $kN_0^* = 1 \times 10^6/\text{sec}$ and $\lambda = 5 \times 10^4/\text{sec}$. The excellent fit of the curve to these data gives considerable confidence to the interpretation and to the parameters derived from the data. However, it must be emphasized that these parameters are based on very limited data and that further data need to be analyzed to confirm these results.



SA-1925-12

FIGURE 9 PLOT OF INVERSE OF INTENSITY VERSUS TIME FOR MOLECULAR RADIATION AT 4570Å

We cannot evaluate the rate k without a knowledge of the initial density N_O^* . If we assume N_O^* is $10^{17}/\text{cm}^3$, then $K = 10^{-11} \text{ cm}^3/\text{sec}$, which is a very reasonable value for a reaction between two excited molecules. From our estimate of the energy deposition by the electrons, we obtained an initial density of $6 \times 10^{17}/\text{cm}^3$, but it is expected that this population will be reduced by electron deactivation, which will be important initially while the electron density is high. We cannot evaluate the electron deactivation processes to obtain a realistic estimate of N_O^* , because neither the electron densities nor the deactivation rate constants are known. We intend in the near future to determine the excimer density from a measurement of the absolute emission intensity, since the transition probability is now known. We also plan to measure the electron density as a function of time following the excitation pulse to evaluate the electron deactivation.

An understanding of the problems described above is essential to a complete evaluation of the lasing possibilities of the Hg continuum band. We now have sufficient information, however, to calculate the density of excimers required to provide a given gain at 4570 \AA . The optical gain equation is

$$G = \frac{\lambda^3}{8\pi c} \frac{\lambda}{\Delta\lambda} A[\text{Hg}_2^*] \quad , \quad (15)$$

where $\Delta\lambda$ is band halfwidth, which in this case is about 600 \AA , and A is the transition probability for which we use our measured value of $5 \times 10^4/\text{sec}$. To obtain a gain of $10^{-2}/\text{cm}$ requires a Hg_2^* concentration of $2 \times 10^{17}/\text{cm}^3$.

As indicated in the discussion above, a density of this order appears possible and may even be attained with our Febetron source, but a more definitive evaluation of the possibilities for an Hg association laser will have to await further measurements.

V CONCLUSIONS

We have described a model of the kinetic processes occurring in a high-pressure Hg gas excited by an electron pulse, as well as an experimental program undertaken to determine some of the many unknown rate constants and transition probabilities of the processes entailed. The experimental program has recently yielded considerable data which have been evaluated only qualitatively at present, but two important results have been obtained from them. The first is a radiative lifetime of 20 microsec for the molecular radiation at 4570 \AA , and the second is that at high densities the molecules are deactivated due to bi-excimer collisions. Photographic spectra also indicate that for our experimental conditions the main continuum spectral band has a half-width of approximately 600 \AA centered near 4570 \AA .

Our results are not yet sufficiently detailed to allow a definitive evaluation of Hg_2 as a laser medium. However, we can determine the optical gain to be $5 \times 10^{-20}/\text{cm}$ for each excited molecule/ cm^3 , or $0.01/\text{cm}$ for 2×10^{17} molecules/ cm^3 . Additional measurements and calculations are continuing to determine the feasibility of achieving excited molecule populations of this magnitude.

REFERENCES

1. R. J. Carbone and M. M. Litvak, J. Appl. Phys. 39, 2413 (1968).
2. A. V. Phelps, unpublished J. I. L. A. report No. 110, University of Colorado, Boulder, Colorado, Sept. 15, 1972.
3. Spectroscopic Data Relative to Diatomic Molecules, B. Rosen, editor (Pergamon Press, New York, 1970), p. 203-5.
4. J. C. McConnell and B. L. Moiseiwitsch, J. Phys. B, Ser. 2, Vol. 2, 821 (1969).
5. W. Finkelberg and Th. Peters, Kontinuierliche Spektren, in Handbuch Der Physik Vol. XXVIII, S. Flugge, ed., Springer-Verlag, Berlin (1957).

MOLECULAR FORMATION IN ELECTRON-EXCITED
HIGH PRESSURE RARE GASES

by

D. C. Lorents
Stanford Research InstituteIntroduction

Basov¹ suggested in 1961 that stimulated emission in the uv range might be realized by utilizing the well known continuum emission from inert liquids and solids excited by energetic charged particles. Since then, he and his coworkers have reported observations of stimulated emission in the 1700 to 1800 Å range in liquid Xe.² More recently, Koehler et al.³ reported strong evidence of stimulated emission in high pressure, electron-excited gaseous Xe. Luminescence of inert gases and liquids excited by electrons has been studied in several laboratories, and surprisingly high energy conversion efficiencies have been reported.³⁻⁵ These observations point to a very real possibility for designing practical and efficient uv lasers using inert gases excited by high energy electrons.

The energy deposited by a fast electron stopped in a high pressure inert gas initially creates ions and electrons and excited atoms. Through rapid recombination processes, the ions and electrons are transformed to excited atoms, which associate with ground state atoms to form excited molecules. At high densities, these molecules rapidly relax to the lowest stable excited state, where they are trapped until they radiate

to the ground state. Since the minima in the potentials of the excited molecules lie at internuclear separations where the ground state is strongly repulsive, the molecules dissociate immediately upon radiating, and no appreciable ground state population of molecules can exist. Molecular state structure of this type is characteristic of van der Waals molecules and should make possible the operation of a new class of lasers based on their unique properties.

Structure of Inert Gas Molecules

Van der Waals molecules are formed from atoms with closed shells, but the interaction between these atoms in the ground state is basically repulsive, except for a very weak attractive interaction at large separations. If one of the atoms is excited, however, the character of the interaction changes, and rather strongly bonding states can result, having equilibrium separations much smaller than that of the ground state. Except for He, the excited state structure of the molecules is not well established, but Mulliken⁶ has constructed a set of estimated potential curves for the lower excited states of Xe_2 . Xe_2 absorption measurements⁷ confirm these curves for internuclear separations larger than the excited state minima. The molecular structure of Kr_2 and Ar_2 are similar to that of Xe_2 , as confirmed⁸ by absorption measurements in Ar_2 . The lowest pair of bound excited states of Xe_2 are the $a^3\Sigma_u^+$ and $A^1\Sigma_u^+$, formed respectively from the association of a ground state 1S_0 atom with an excited 3P_2 or a 3P_1 atom. Direct evidence for identification of the 1700 Å band in Xe_2 with the A-X transition has been established by the observation that Xe optically pumped to the 3P_1 state at high pressures fluoresces at 1700 Å.⁹

Emission spectra from the inert gases have been observed in discharges at low pressures and at high pressures excited by electron and ion beams. Above 1.0 atm, the only observed emission is the single uv

band corresponding to the a-X and A-X transitions. At these pressures, molecules formed in upper excited states are evidently rapidly quenched to the lowest excited states by collisions. The quenching mechanism is suggested in the potential energy diagram for Xe_2 , which shows several possible curve crossings that permit radiationless transitions between states and provide a means for lowering the level of excitation. However, it is important to note that no curve crossings with the ground state occur, so that quenching to the ground state by atom collisions is very improbable.

Electron Energy Deposition

The efficiency of conversion of energy from the electrons to radiation in the molecular band is evaluated from the ratio of the mean energy of the emission band to the mean level of initial excitation. This estimate is easily made in Ar, where the energy deposition processes by electrons have been analyzed in detail.¹⁰ The similarities in energy level structure of the rare gases Ar, Kr, and Xe, together with the similarities in the excitation cross sections, permit the assumption that the partitioning of energy among ions, excited states, and secondary electrons in Kr and Xe will be close to that of Ar. Using the known energy loss per ion pair, W , which can be related through the equation

$$W = \frac{E}{n_i} = \epsilon_i + \epsilon_{se} + \frac{n_{ex}}{n_i} \epsilon_{ex}$$

to the mean excitation energy, ϵ_{ex} , the ionization potential, ϵ_i , and the mean secondary electron energy ϵ_{se} , we can calculate n_{ex}/n_i , the ratio of excited atoms to ions produced by the electron. The efficiency, R , of producing molecular radiation by high energy electron bombardment can then be calculated by assuming complete recombination and molecular association:

$$R = \frac{n_{ex}}{n_{ex} + n_i} \cdot \frac{h\nu_m}{\epsilon_{ex}} + \frac{n_i}{n_{ex} + n_i} \cdot \frac{h\nu_m}{\epsilon_i + \epsilon_{se}},$$

where $h\nu_m$ is the mean energy of the molecular radiation. The results are tabulated in Table A-1.

Table A-1

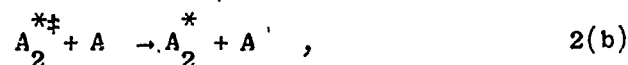
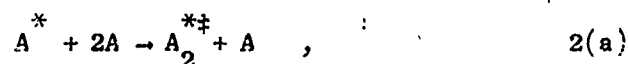
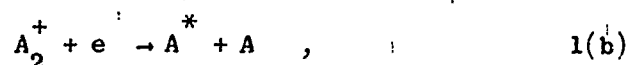
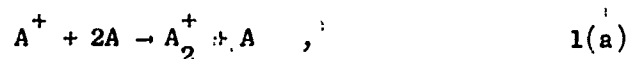
EFFICIENCY OF PRODUCING MOLECULAR RADIATION
BY HIGH ENERGY ELECTRON BOMBARDMENT

	ϵ_i	ϵ_{ex}	ϵ_{se}	W	$h\nu$	$\frac{n_i}{n_{ex} + n_i}$	R
	(eV)	(eV)	(eV)	(eV)	(eV)	(percent)	(percent)
Ar	15.7	13.2	6.9	26.2	10	78%	53%
Kr	14.0	11.6	6.1	24.3	8.7	74	52
Xe	12.1	9.8	5.3	21.9	7.5	69	54

R represents the total radiative efficiency of the molecular bands under high pressure conditions, provided the molecules are not deactivated by other processes. Deactivation by collisions with slow electrons could be important at high electron densities. Thus, R should be regarded as an upper limit to the efficiency that can be expected in these gases. Measurements in Ar at 400 torr excited by 4 MeV protons yielded a 29% efficiency;⁴ Koehler et al.³ found the efficiency in Xe at 250 psi to lie between 12 and 25%.

Reaction Rates

To attain high efficiency, it is necessary that the recombination and relaxation processes be rapid enough to populate the active state before appreciable spontaneous radiation occurs. The molecular formation is controlled by two sets of important recombination and associative processes, described by the following simplified set of reactions:



where the asterisk indicates electronic excitation and the double dagger indicates vibrational excitation. Rate constants for most of these reactions in the inert gases are known or can be estimated reasonably well. Because of the three-body collisions involved, high pressures are needed to obtain sufficiently rapid rates. The spontaneous radiative lifetimes of these molecules are not well established, but Koehler et al.³ obtained a lifetime of 20 ns for Xe₂, whereas a 2.8 μs lifetime is reported¹¹ for Ar₂.

The rates for the three-body ion association, Reaction 1(a), are reasonably well established¹² and indicate that at 10 atm the A₂⁺ formation time is about 0.1 nsec. We can therefore expect that a major electron-ion recombination process will be dissociative recombination. If the electron concentration becomes sufficiently high and they are rapidly thermalized, however, dielectronic recombination (A⁺ + 2e → A^{*} + e) can be important. The electrons start with a mean energy of several eV and cool rapidly (cooling time ~ 2 to 3 nsec)¹³ by momentum transfer collision with ground state atoms to an energy on the order of 1 eV. At

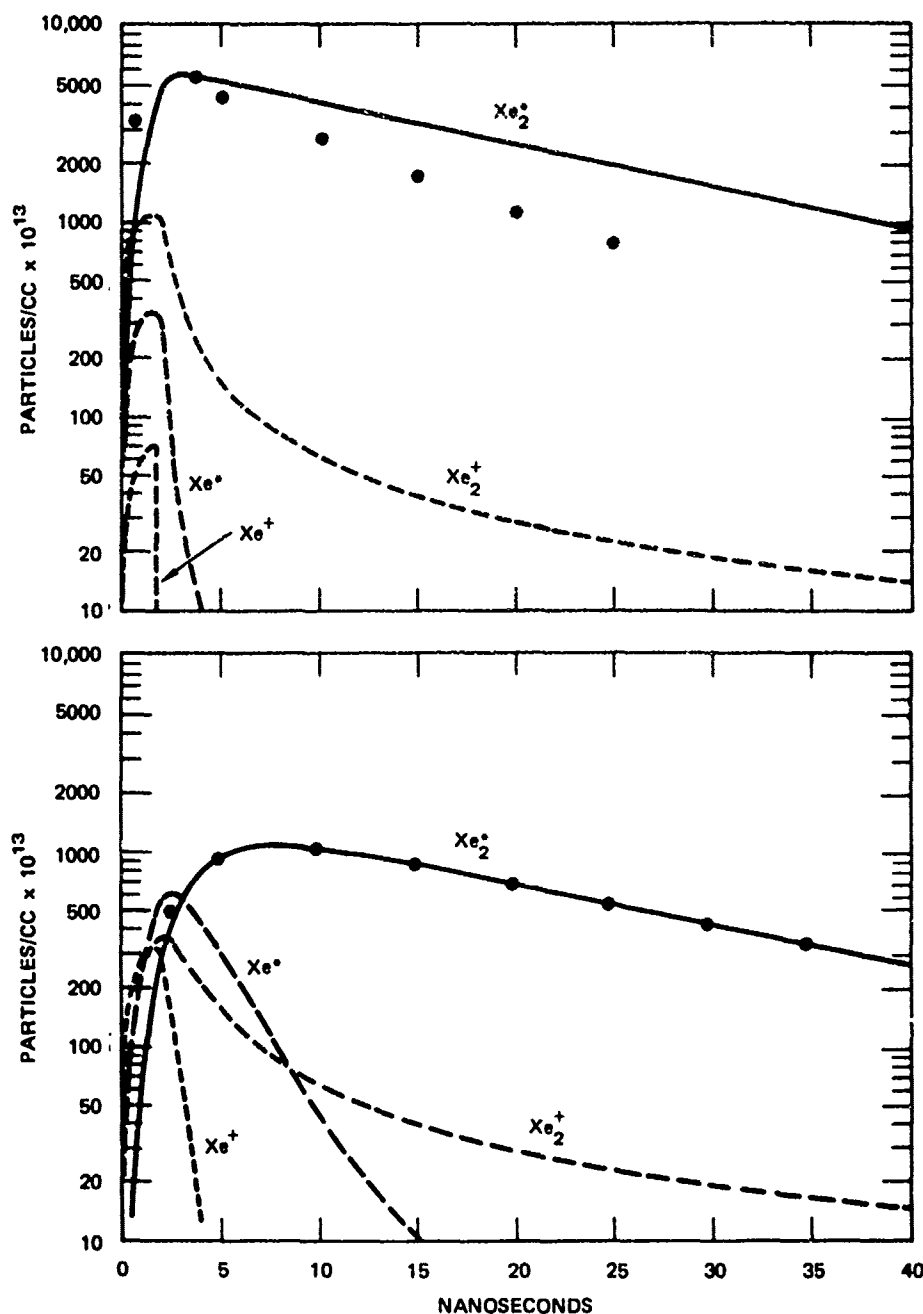
this energy, the electron cooling rate becomes slow because of the deep minimum in the cross section near 0.5 eV. At temperatures above 0.5 eV, the dissociative mechanism clearly dominates the recombination for the electron densities expected in this case.¹⁴ For example, at an electron density of $10^{16}/\text{cm}^3$, the dissociative recombination time for 1 eV electrons in Ar is 1 nsec.

Formation of the excited molecules occurs by three-body associative reactions of an excited atom and two ground state atoms. Atom-atom deactivation processes for the lowest excited states in Ar¹⁵ and Kr¹⁶ are slower than the three-body rates for association at 10 atm. Thus, the newly formed molecules will be found in various electronic levels and will also be highly excited vibrationally. An important consideration that then arises is, by what mechanisms and how rapidly this electronic and vibrational excitation relaxes to the lowest excited state. In symmetric systems, a vibrationally excited molecule in a cold gas of atoms will rapidly be cooled to the ambient level by atom-atom exchange collisions, as in the case of liquids.¹⁷ The electronic relaxation can occur by means of curve crossing interactions between attractive states and repulsive states that allow the excitation to flow down to the lowest excited atom states. These predissociative types of reactions will occur most probably when the molecule is in a vibrational level near the crossing point, but they may also be triggered by the perturbation of a collision. This relaxation is evidently very rapid, since the emission band becomes independent of pressure above a few atmospheres.

The formation times for three-body associative reactions from the metastable levels in Ar, Kr, and Xe at 10 atm are in the range of 0.2 to 2 nsec. The relaxation rates are not known, but the formation times for Xe₂ indicate extremely rapid relaxation (at 10 atm the formation plus relaxation time is ≤ 2 nsec). Koehler et al.³ observe the formation rate

to be proportional to pressure to the 1.7 power, indicating a probable two-step process of three-body association, followed by two-body relaxation. Such a process is also indicated by Thonnard and Hurst's measurements in Ar.¹¹

We have solved the rate equations for Reactions (1) and (2) to determine the time-dependent concentrations of ions, excited atoms, and molecules. The excitation pulse is characteristic of that used in the experiments of Koehler et al. (2000 A/cm² at 0.5 MeV, 2 nsec pulse) and is estimated to produce ions at the rate of $2 \times 10^{15} \text{ cm}^{-3} \text{ nsec}^{-1} \text{ atm}^{-1}$ and excited atoms at the rate of $8 \times 10^{14} \text{ cm}^{-3} \text{ nsec}^{-1} \text{ atm}^{-1}$. The results of this simple model for Xe are shown in Figure A-1 at 40 and 165 psi, together with the data of Koehler et al. These curves clearly indicate the strong pressure dependence in the decay rates of ions and excited atoms and in the buildup of molecules. The emission decay rate is constant for all pressures up to 115 psi, and the clear increase in the observed rate of decay of the emission at 165 psi is evidently due to superradiance. Since the electron densities at the two pressures shown in Figure A-1 are identical after 5 nsec, the increased molecular decay rate cannot be due to an increased electron deactivation rate. A simple computation of the single pass gain for an estimated 2 cm path length through Xe at 165 psi with an excited state density of $5 \times 10^{16} \text{ cm}^{-3}$ gives nearly unity, clearly a superradiant condition.



SA-2018-1

FIGURE A-1 CALCULATED TIME DEPENDENT DENSITIES OF Xe^+ , Xe_2^+ , Xe^* AND Xe_2^* AT 40 psi (LOWER CURVES) AND 165 psi (UPPER CURVES). The rate coefficients used in these calculations were $k(1a) = 3 \times 10^{-40} \text{ cm}^6/\text{nsec}$, $k(1b) = 1.8 \times 10^{-16} \text{ cm}^3/\text{nsec}$, $k(2a) = 1 \times 10^{-40} \text{ cm}^6/\text{nsec}$, $k(2b) = \infty$, Radiative decay rate = $5 \times 10^{-2}/\text{nsec}$. The solid points are from the data of Koehler et al. normalized to the Xe_2^* density.

REFERENCES

1. N. G. Basov, IEEE J. Quant. Elect. 2, 354 (1966).
2. N. G. Basov, V. A. Danilychev, and Yu. M. Popov, Kvantovaya Electron (USSR) 1, 29 (1971), [Trans. in Soviet J. Quant. Elect. 1, 18 (1971)].
3. H. A. Koehler, L. J. Ferderber, D. L. Redhead, and P. J. Ebert, Appl. Phys. Lett. (to be published).
4. T. E. Stewart, G. S. Hurst, T. E. Dortner, J. E. Parks, F. W. Martin, and H. L. Weidner, J. Opt. Soc. 60, 1290 (1970).
5. J. Jortner, L. Meyer, S. A. Rice, E. G. Wilson, J. Chem. Phys. 42, 4250 (1965).
6. R. S. Mulliken, J. Chem. Phys. 52, 5170 (1970).
7. M. C. Castex and N. Damany, Chem. Phys. Lett. 13, 158 (1972).
8. Y. Tanaka and K. Yoshino, J. Chem. Phys. 53, 2012 (1970).
9. C. E. Freeman, M. J. McEwan, R.F.C. Claridge and L. F. Phillips, Chem. Phys. Lett. 10, 530 (1971).
10. L. R. Peterson and J. E. Allen, J. Chem. Phys. 56, 6068 (1972).
11. N. Thonnard and G. S. Hurst, Phys. Rev. A 5, 1110 (1972).
12. E. W. McDaniel, V. Cermak, A. Dalgarno, E. E. Ferguson, and L. Friedman, Ion-Molecule Reactions, Wiley-Interscience (1970) pp. 338-9.
13. L. S. Frost and A. V. Phelps, Phys. Rev. 136, A1538 (1964).
14. J. N. Bardsley and M. A. Biondi in Advances in Atomic and Molecular Physics, Vol. 6, D. R. Bates and I. Esterman eds., Academic Press (1970).
15. E. Ellis and N. D. Twiddy, J. Phys. B, 2, 1366 (1969).
16. R. Turner, Phys. Rev. 158, 121 (1967).
17. M. Martin, J. Chem. Phys. 54, 3289 (1971).

Appendix B

ELECTRON IMPACT CROSS SECTIONS FOR THE ELEMENT MERCURY

by

J. M. Bass, R. A. Berg, A. E. S. Green

Introduction

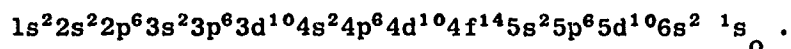
Recent interest in the element mercury for use in an electronically pumped laser has stimulated interest in having a reasonably complete set of electron impact cross sections for this element. The approach in this work is to treat the available experimental data in a semiempirical manner which should allow us to extrapolate from regions in which data are relatively plentiful to those in which they are rare or nonexistent. This basic approach has been applied to a number of gases important in upper atmospheric physics.¹⁻⁷ Most recently the approach has been used on argon by Peterson and Allen⁸ starting from the Born approximation for an electron scattering from an atom.

For laser applications, knowledge of the secondary electron spectrum and its efficiency for regulating various excited levels is of great importance. For this type of analysis, if only the relative populations of the various excited states following the degradation of the energy content of the incident beam are of interest and not the spatial distributions, one needs only the cross sections $\sigma_j(E)$ for exciting state j and the differential cross sections $d\sigma_i(E,T)/dT$ for creating an ion in the state i and ejecting a secondary electron of energy T . We will construct simple but reasonable functional representations of these cross sections from

available data, using these data as a constraint to determine the parameters in the functional representations. Once we have this set of cross sections, we can easily calculate quantities such as the loss function $L(E)$; the ionization yield $J(E)$ or, equivalently, the mean energy to create an ion pair (eV/ion pair); and the excited state populations.

Structure of Mercury

The atomic number of Hg is 80. Its ground state electronic configuration is



It is thus an example of a two-valence electron heavy element. As such, it is difficult to treat theoretically with accuracy. Russell-Saunders coupling breaks down for Hg because of a nonvanishing spin-orbit interaction producing states that are not pure L-S states but singlet-triplet mixtures that allow transitions that normally would be forbidden. In addition, there is an inversion of the singlet-triplet energy levels for D states of the atom. This may be due to configuration interaction or spin-orbit interactions or both. Hg also has another energy level series which was observed by Beutler.⁹ This series is caused by promotion of an electron from the 5d subshell instead of the 6s outer subshell. Most of the energy levels in this series lie above the first ionization limit of 10.4 eV allowing auto-ionization of Hg to take place. Figure B-1 is an energy level diagram of the excited states of Hg caused by the transition of one of the 6s electrons. The values of these energy levels have been taken from Moore's¹⁰ tables and we use the same notation. We note that if the L-S coupling scheme were good for Hg, the Landé interval rule would hold and level structure such as the 7p levels would not be observed.

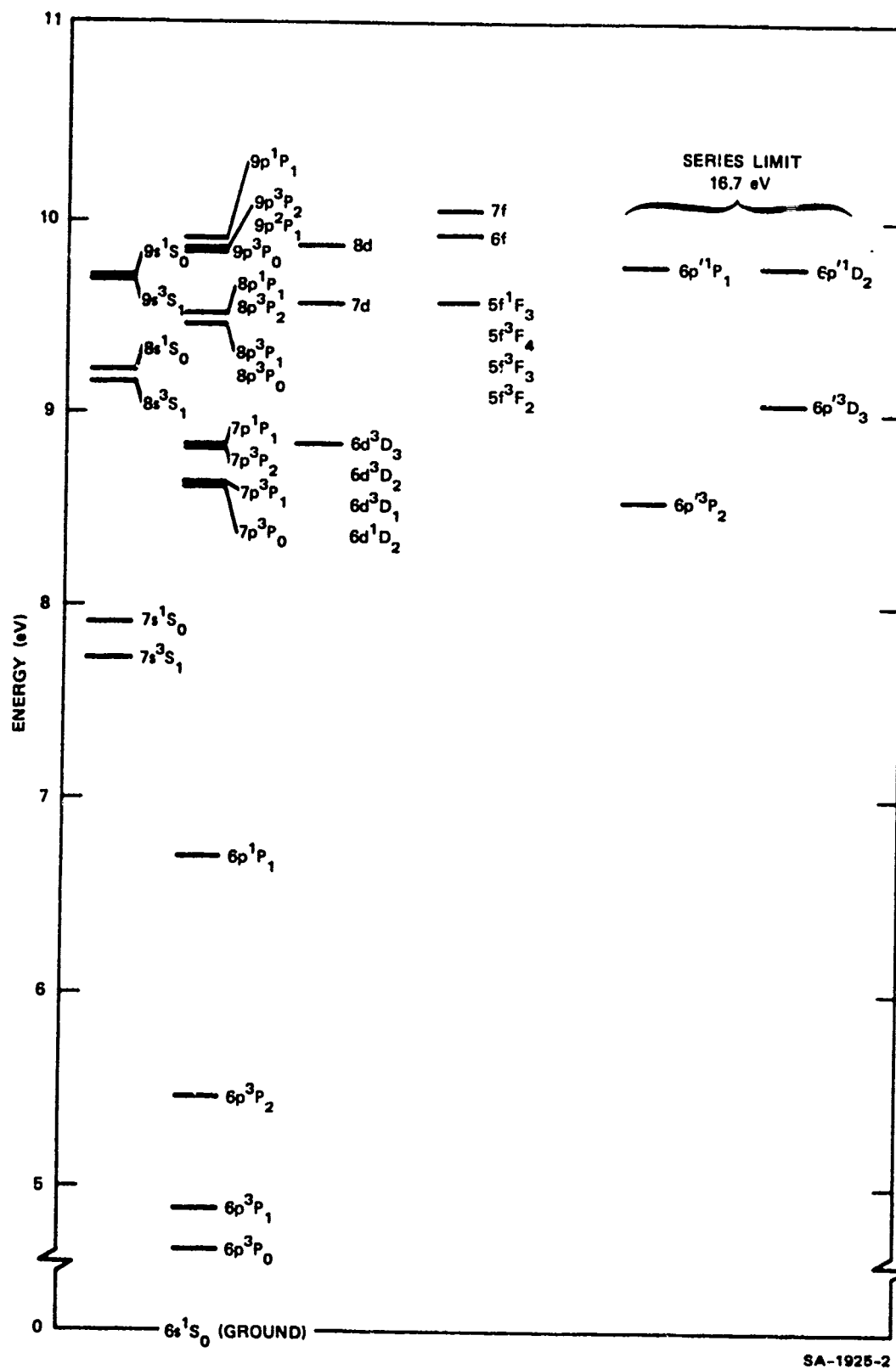


FIGURE B-1 HgI ENERGY LEVELS FROM TABLES OF MOORE¹⁰

Discrete Excitation Cross Sections: Helium Rules

We represent our discrete cross sections by the analytical form

$$\sigma(E) = \frac{q_o f_o c_o}{W^2} \left[1 - \left(\frac{W}{E} \right)^\beta \right]^\nu \left(\frac{W}{E} \right)^\Omega, \quad (1)$$

where $q_o = 6.514 \times 10^{-14} \text{ cm}^2 \cdot \text{eV}^2$, W is the excitation energy; c_o , β , ν , and Ω are fitting parameters for allowed transitions; and f_o is the optical oscillator strength. Since mercury has the same ground state configuration as helium (s^2 outer shell), we expect the cross sections to exhibit similarities. Therefore, we adopt as a first approximation for mercury cross sections the same parameter values as for helium, except for the strength parameters f_o and the excitation energies W .

Measurements of helium cross sections have been collected and reported by Jusick et al.² These cross sections have been fitted to Equation (1). To determine strength parameters f_o , we have computed the generalized oscillator strengths $f(x)$ following Ganas and Green.²¹ These were computed using one-electron wave functions generated by the analytic potential of Green, Sellin, and Zachor,¹¹

$$V(r) = [N\psi - Z]/r; \quad \psi = 1 - \Omega = 1 - [(e^{r/d} - 1)H - 1]^{-1}, \quad (2)$$

where $Z = 80$, $N = Z - 1$, and H and d are adjustable parameters. The parameter values, determined by fitting the potential to Moore's energy levels,¹⁰ averaged over fine structure, were

$$H = 3.5271 \quad ; \quad d = .65547 \quad . \quad (3)$$

For allowed transitions ($6s \rightarrow np$), $f(x)$ is the optical oscillator strength f_o at $x = 0$, while for forbidden transitions ($6s \rightarrow ns$ or nd),

$f(x)/x$ approaches a constant $\bar{\phi}_0$. We thus fit f_0 and $\bar{\phi}_0$ to the expressions;

$$f_0 = \frac{f_0^*}{(n-\delta)^3} \quad ; \quad \bar{\phi}_0 = \frac{\bar{\phi}_0^*}{(n-\delta)^3} \quad . \quad (4)$$

The parameter f_0 for forbidden singlet cross sections was determined by using the same expression for the allowed cross sections (first of the above expressions) but with the quantum defect δ appropriate to the forbidden cross sections (determined by second expression). For triplet cross sections, we used the same f_0 parameter values as for the corresponding singlets. Excitation energies were taken from Moore's tables.¹⁰ Final parameter values are given in Table B-1.

Table B-1

DISCRETE EXCITATION CROSS SECTION
PARAMETERS FOR MERCURY

State	β	ν	Ω	$f_0^* \text{ co}$
ns ¹ S	2.0	1.0	.75	.02730
np ¹ P	1.0	3.0	.75	.07290
nd ¹ D	1.0	1.0	1.00	.00455
ns ³ S	1.0	2.0	4.00	.10500
np ³ P	1.0	2.0	3.00	.06900
nd ³ D	1.0	1.0	2.50	.01360

Ionization Cross Sections

The ionization spectrum of Hg is not well known, since very few angular cross sections are available experimentally. For the purposes of a degradation study of the type that we want to do, however, angular data are not necessary. We do need the so-called doubly differential cross section $S(E,T)$ which is a function of both the incident electron energy E and the energy loss of the ejected electron T . This quantity unfortunately also has not been reported experimentally. A number of experimenters have measured the gross ionization cross section, among them Compton and Van Voorhis,¹² T. J. Jones,¹³ W. Bleakney,¹⁴ P. T. Smith,¹⁵ J. W. Liska,¹⁶ and more recently H. Harrison.¹⁷ The results of most of them have also been reported in a review article by Kieffer and Dunn.¹⁸

As a result of previous work on the subject of ionization, the following functional form has been found as a reasonable approximation to $S(E,T)$ ¹⁹

$$S(E,T) = A(E) \frac{\Gamma(E)^2}{[T - T_o(E)]^2 + \Gamma(E)^2}, \quad (5)$$

where

$$A(E) = 10^{-16} \text{ cm}^2 \frac{K}{E} \ln \left(\frac{E}{J} \right)$$

$$\Gamma(E) = \frac{E}{s(E + \Gamma_b)} \quad (6)$$

$$T_o(E) = T_s - \frac{T_a}{E + \Gamma_b}$$

The constants in these equations are to be given by fits to experimental data. The form for $S(E,T)$ has the favorable property that it can be analytically integrated over T , thus giving the total ionization cross section $\sigma_i(E)$. This results in a total ionization cross section given by

$$\sigma_i(E) = A\Gamma[\tan^{-1}(T_m - T_o)/\Gamma + \tan^{-1}(T_o/\Gamma)] \quad , \quad (7)$$

where $T_m = \frac{1}{2}(E - I)$, and I is the ionization threshold. We have done a nonlinear least squares fit of this function to the gross ionization cross sections, treating the constants as parameters, to obtain the function $S(E,T)$.

Since there was considerable spread in the reported values of gross ionization cross sections, we have taken the data of Bleakney¹⁴ as an upper limit and those of Smith¹⁵ and Liska¹⁶ as a lower limit. Table B-2 has the parameter values obtained from these two fits. Figure B-2 shows the data and our fits to them.

Table B-2

PARAMETERS FOR FITS TO MERCURY
IONIZATION CROSS SECTIONS

	Smith ¹⁵ -Liska ¹⁶	Bleakney ¹⁴
K	6.899	12.775
J(eV)	5.180	2.396
Γ_s (eV)	7.805	22.697
Γ_b (eV)	-6.680	-6.680
T_s (eV)	-8.830	-8.830
T_a (eV)	1000.000	1000.000
T_b (eV)	10.434	10.434

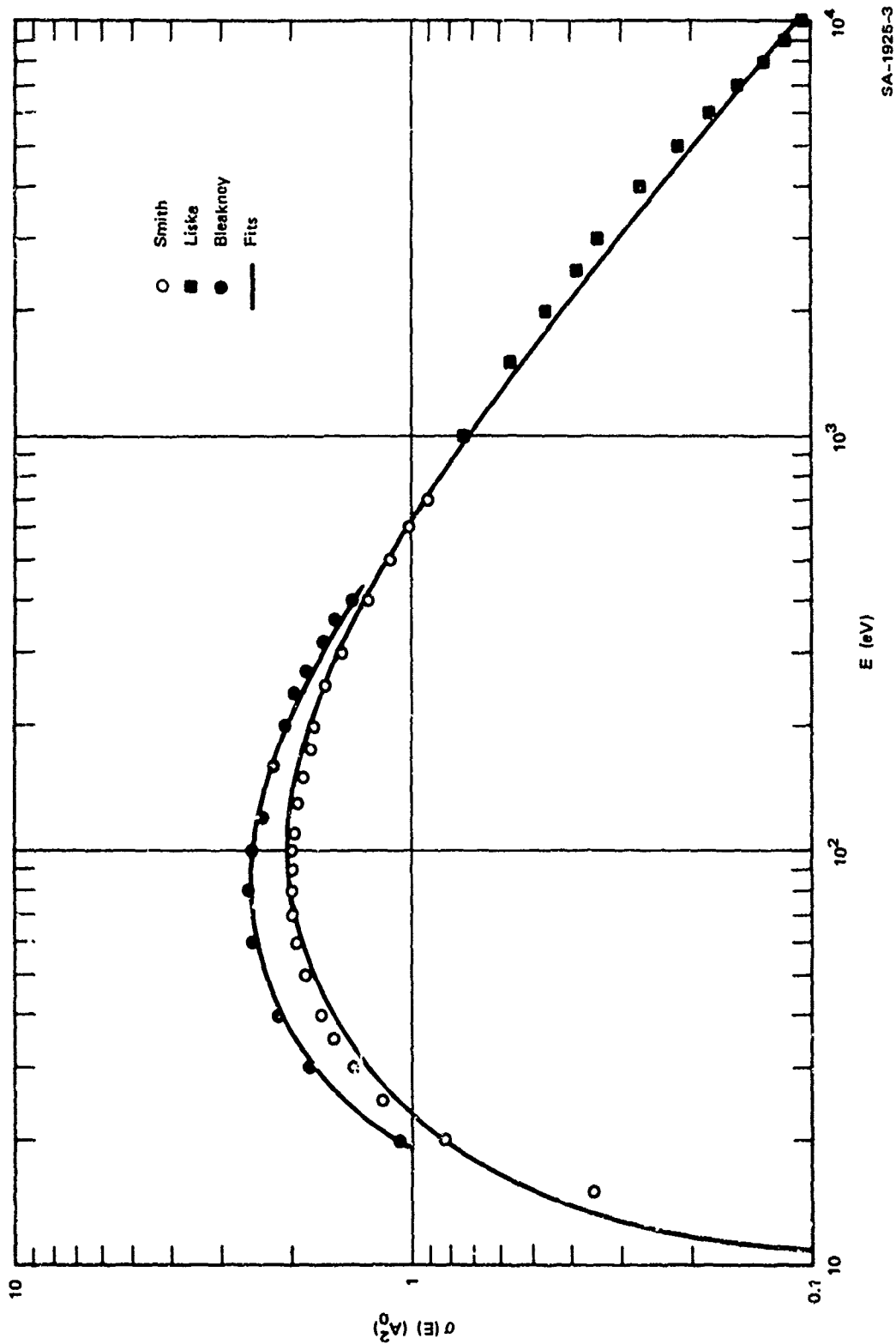


FIGURE B-2 FITS TO HgI IONIZATION CROSS SECTION

Energy Deposition

Once a complete set of electron impact cross sections is known, it is possible to carry out an energy deposition analysis in which we determine the energy deposited in various excitations (or, equivalently, the number of such excitations) as a result of the complete degradation of an electron with given initial energy. To do this, we first calculate the loss function

$$L(E) = - \frac{1}{n} \frac{dE}{dx} , \quad (8)$$

where n is the number density of the gas. The expression for $L(E)$ in terms of all the cross sections is given most recently by Peterson and Allen⁸ and will not be repeated here. We then calculate the secondary spectrum,

$$n(E,T) = \sum_i \int_{2T+I_i}^E \frac{S_i(E',T)}{L(E')} dE' , \quad (9)$$

where I_i is the ionization threshold for the i^{th} ionization continuum and $S_i(E',T)$ is the differential cross section for production of secondaries with energy T . Finally we may calculate the population of the j^{th} excited state

$$j_j(E) = \int_{W_j}^E \frac{\sigma_j(E')}{L(E')} dE' + \int_0^{(E-I_0)/2} j_j(T) n(E,T) dT , \quad (10)$$

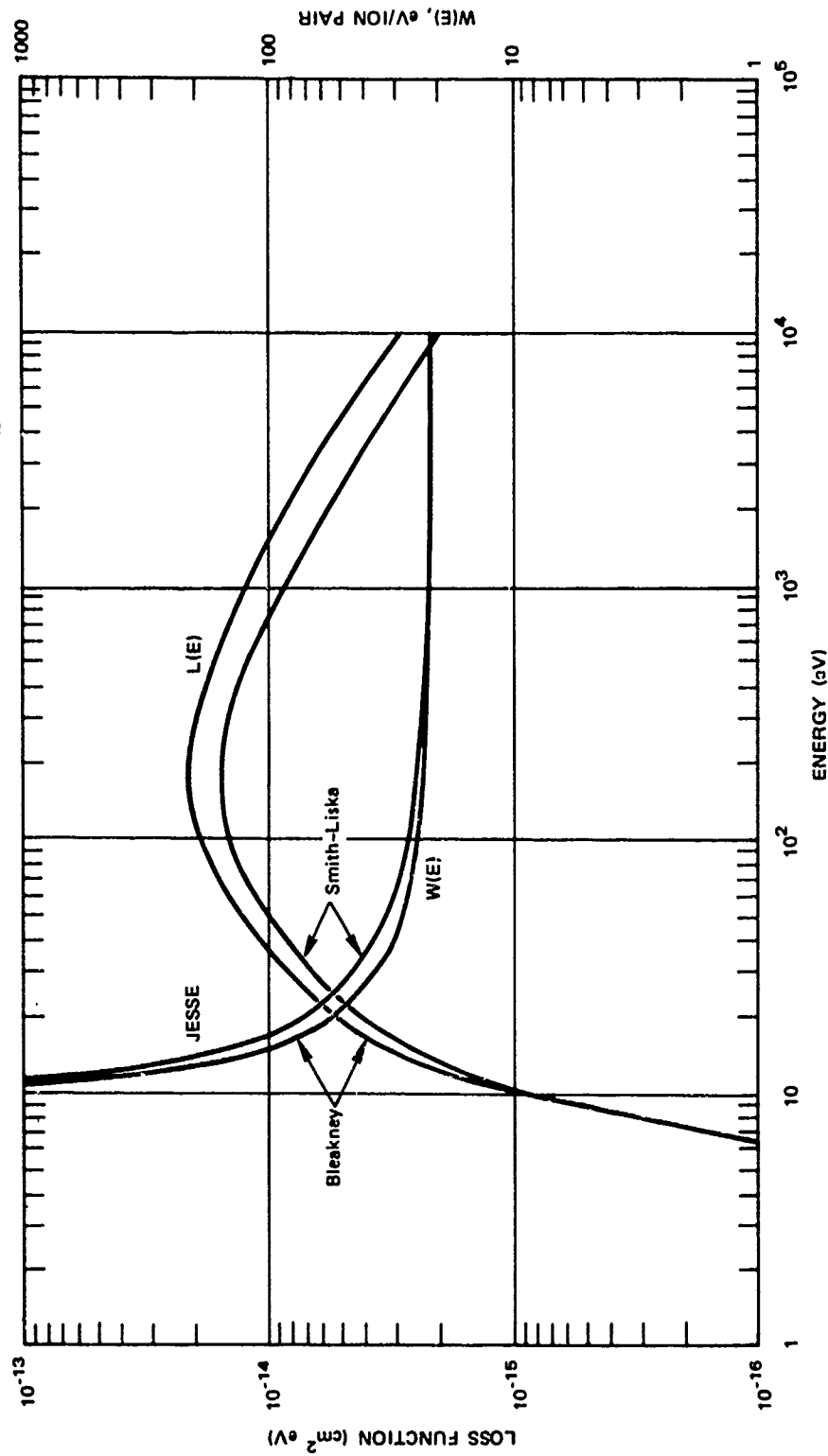
where σ_j is the excitation cross section for this state and I_0 is the lowest ionization threshold. Here the first term represents the contribution from the primary electron alone, while the second term gives the contribution resulting from the secondaries produced by ionization by the primary.

This analysis was first carried out using the "Helium Rules" discrete excitation cross section and both the Smith-Liska and Bleakney ionization cross sections. The loss functions and eV/ion pair, $W(E)$, for these two cases are plotted in Figure B-3. We see that in both cases W_1 at high energy is in good agreement with the experimental result of 23.6 eV/ion pair obtained by Jesse.²⁰

In Figure B-4 we plot the efficiencies

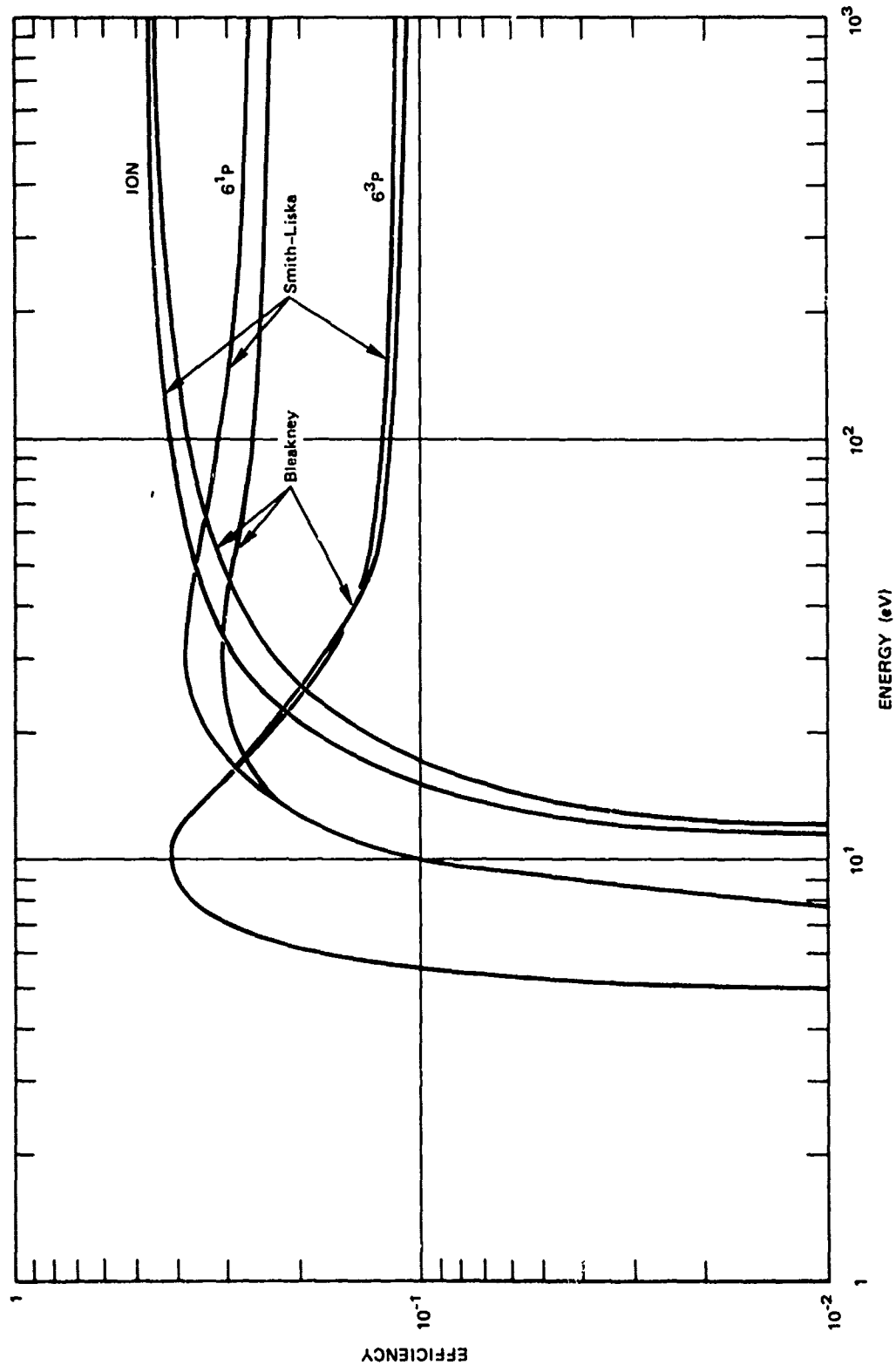
$$\epsilon_j(E) = \frac{W_j}{E} \quad (11)$$

for depositing energy in various discrete excited states. Of considerable interest for laser applications is the 6^3P state, since atoms in this state may combine with atoms in the ground state to form stable diatomic molecules.



SA-1925-4

FIGURE B-3 TOTAL LOSS FUNCTION AND eV/ion PAIR FOR MERCURY



SA-1925-6

FIGURE B-4 EFFICIENCIES FOR DEPOSITION OF ELECTRON ENERGY INTO THE 6^1P AND 6^3P STATES OF MERCURY

References

1. A. E. S. Green and S. K. Dutta, J. Geophys. Res. 72, 3933 (1967).
2. A. T. Jusick, C. E. Watson, L. R. Peterson, and A. E. S. Green, J. Geophys. Res. 72, 3943 (1967).
3. R. S. Stolarski, V. A. Dulock, Jr., C. E. Watson, and A. E. S. Green, J. Geophys. Res. 72, 3953 (1967).
4. C. E. Watson, V. A. Dulock, Jr., R. S. Stolarski, and A. E. S. Green, J. Geophys. Res. 72, 3961 (1967).
5. D. J. Strickland and A. E. S. Green, J. Geophys. Res. 74, 6415 (1969).
6. A. E. S. Green, J. J. Olivero, and R. W. Stagat, Proc. Intern. Symp. Biophys. Effects Radiation Quality, Lucas Heights, Australia, 1971.
7. W. T. Miles, R. Thompson, and A. E. S. Green, J. Appl. Phys. 43, 678 (1972).
8. L. R. Peterson and J. E. Allen, Jr., J. Chem. Phys. 56, 6038 (1972).
9. H. Beutler, Z. Physik 86, 710 (1933).
10. C. E. Moore, "Atomic Energy Levels, "Nat. Bur. Std. (U. S.) Circ. No. 467 (1949).
11. A. E. S. Green, D. L. Sellin, and A. S. Zachor, Phys. Rev. 184, 1 (1969).
12. K. T. Compton and C. C. Van Voorhis, Phys. Rev. 26, 436 (1925); Phys. Rev. 27, 724 (1926).
13. T. J. Jones, Phys. Rev. 29, 822 (1927).
14. W. Bleakney, Phys. Rev. 35, 139 (1930).
15. P. T. Smith, Phys. Rev. 37, 808 (1931).
16. J. W. Liska, Phys. Rev. 46, 169 (1934).
17. H. Harrison, "The Experimental Determination of Ionization Cross Sections of Gases under Electron Impact", thesis. The Catholic University of America Press, Washington, D. C., (1956).

18. L. J. Kieffer and G. H. Dunn, Rev. Mod. Phys. 38, 1 (1966).
19. A. E. S. Green and T. Sawada, J. Atmos. Terr. Phys. (to be published, 1972).
20. W. P. Jesse, J. Chem. Phys. 55, 3603 (1971).
21. P. S. Ganas and A. E. S. Green, Phys. Rev. A 4, 182 (1971).